

Figures/preliminary results

Figure 1 Initial cryoEM analysis of ACE. A. SDS page of purified ACE. B. 3D classification of ACE. Extra-densities are mostly from N-linked glycosylations. It is worth noting that ACE-C domains have substantially poor density in comparison to ACE-N, suggesting the denaturation or high structural heterogeneity.

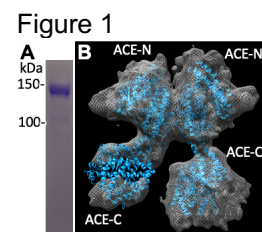


Figure 2 3D classification from the optimized buffer condition that better maintains ACE stability. Of three classes, the most common structure (60% particle) is consistent with that contains only two ACE-N domains. The second (25%) is that contains both ACE-N domains and only one ACE-C. The least one is the dimeric ACE that contains all four ACE catalytic domains. Our data suggests the preferential denaturation of ACE-C domains.

Figure 2

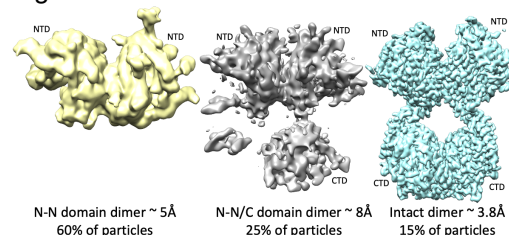


Figure 3 Structural heterogeneity analysis of ACE. A. Domain organization of ACE. B. Comparison of 2D classes from Vitrobot and Chameleon prepared datasets demonstrating higher proportion of four domain dimer classes in Chameleon datasets. C. 3D reconstructions of ACE. Chameleon permitted higher resolution reconstruction and allowed identification of three distinct conformational states.

Figure 3

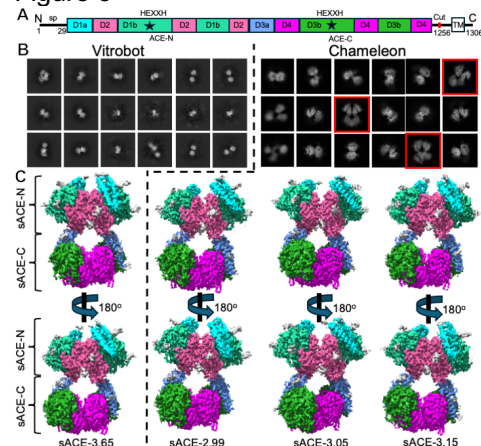


Figure 4

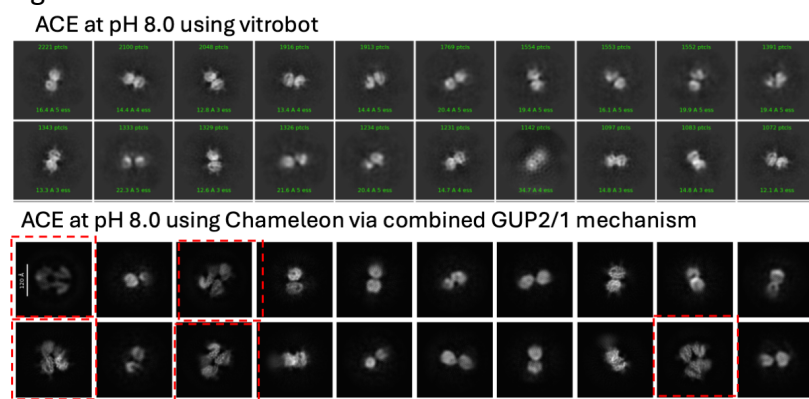


Figure 4 Comparison of top 2D classes of human ACE extracellular region at pH 8.0 with micrographs prepared by grids using vitrobot versus that by chameleon done by NCCAT via combined GUP 1 & 2 programs. None of 2D classes has the expected four-domain structure from vitrobot prepared grid, thus we could not obtain 3D structure of four-domain

extracellular region of ACE. Under the same condition and using chameleon for grid preparation, we have obtained 2D classes that have four-domain feature marked by red box. At pH 8.0, the physiological relevant substrate, amyloid beta has the reasonable solubility, which should allow us to assess the structure of amyloid beta bound ACE structure.

Figure 5 Coulomb potential map (top) and FSC curves (bottom) of three distinct classes of extracellular region of ACE dimer at pH 8.0 using grid prepared by chameleon.

Figure 5

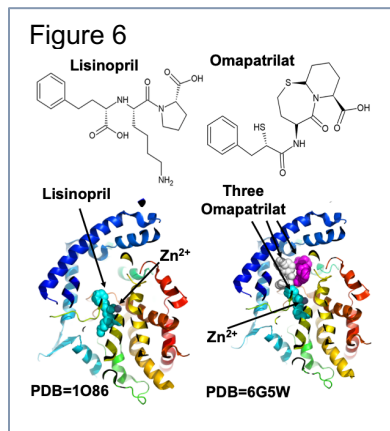
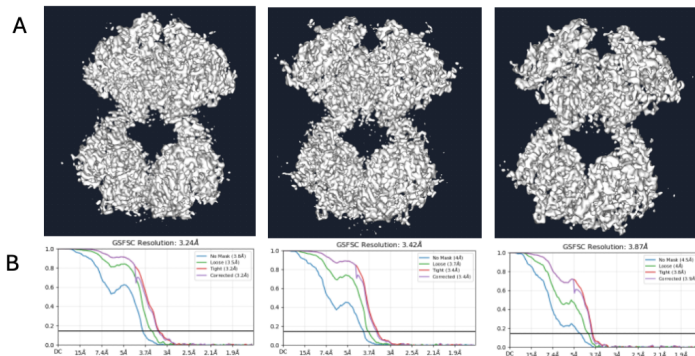


Figure 6 Structures of lisinopril and omapatrilat (top) and their complex with ACE-C (bottom). X-ray crystallographic analysis reveals that while one Lisinopril molecule binds the catalytic pocket of ACE-C, three omapatrilat molecules bind the catalytic pocket of ACE-C.